STATISTICAL WAVE FIELD THEORY: MAIN RESULTS

Roland Badeau[1]

[1] *Laboratoire Traitement et Communication de l'Information, Télécom Paris, Institut Polytechnique de Paris*

This paper is a revised version of the authors' submitted manuscript that was peer-reviewed by at least two anonymous reviewers.

Abstract

The statistical wave field theory mathematically establishes the statistical laws of the solutions to the wave equation in a bounded domain. It provides the closed-form expressions of the power distribution and the correlations of the wave field jointly over time, frequency and space, which hold at high frequency and after many reflections, in terms of the geometry and the specific admittance of the boundary surface. This paper summarizes the main results of the theory.

Keywords: *statistical physics, wave equation, Helmholtz equation, reverberation*

1. Introduction

In a recent series of papers [1]–[5], we introduced the statistical wave field theory, which establishes mathematically the statistical laws of the solutions to the wave equation in a bounded domain, under mild conditions on the domain's geometry. This theory may find applications in various science fields, including room acoustics, electromagnetic theory, and nuclear physics. In room acoustics, it permitted us to retrieve the previously known statistical properties of late reverberation in mixing rooms. However, this new theory has proved to be more general, more accurate, and more informative than the existing approaches, and its prediction of the reverberation time has been verified by experiment [6]. This article is intended for readers who wish to learn about the main findings of the theory, without having to delve into its subtleties. This paper is structured as follows. In Sec. 2, we recall a few fundamental notions regarding wave propagation. In Sec. 3, we list the three mathematical assumptions on which the theory relies, and briefly present the Wigner time-frequency distribution. Then in Sec. 4, we summarize the main results of the theory that hold in isotropic wave fields, before addressing the general case of anisotropic wave fields in Sec. 5. Finally, in Sec. 6 we summarize the main contributions and we propose a few perspectives for future work.

Corresponding author: *roland.badeau@telecom-paris.fr.*

This work was funded by the European Union (ERC, HI-Audio, 101052978). Views and opinions expressed are however those of the author(s) only and do not necessarily reflect those of the European Union or the European Research Council. Neither the European Union nor the granting authority can be held responsible for them.

2. Fundamentals of waves revisited

This section summarizes a few fundamental notions regarding wave propagation that are needed in the rest of the paper. Most of these notions are well-known and are described for instance in [7].

2.1. Main definitions

In a connected open domain $V \subseteq \mathbb{R}^3$, the homogeneous wave equation states that

$$\Delta p(\boldsymbol{x}, t) - \frac{1}{c^2}\frac{\partial^2 p(\boldsymbol{x},t)}{\partial t^2} = 0, \tag{1}$$

where $p(\boldsymbol{x}, t)$ is the wave amplitude at position $\boldsymbol{x} \in V$ and time $t \in \mathbb{R}$, Δ is the Laplacian, and c is the propagation speed. Applying the Fourier transform w.r.t. time to Eq. (1) yields the Helmholtz equation:

$$\Delta \phi(\boldsymbol{x}) + 4\pi^2 k^2 \phi(\boldsymbol{x}) = 0, \tag{2}$$

where the scalar $k = \frac{f}{c}$ is the *wave number* and f denotes the frequency. Any solution ϕ to Eq. (2) is an eigenfunction of the Laplacian, of eigenvalue $-4\pi^2 k^2$. Given a point source position $\boldsymbol{x}_0 \in V$ and a space position $\boldsymbol{x} \in V$, the *room impulse response* (RIR) $h(\boldsymbol{x}, \boldsymbol{x}_0, t)$ is defined as the unique causal solution to the following inhomogeneous wave equation: $\forall t \in \mathbb{R}$,

$$\Delta h(\boldsymbol{x}, \boldsymbol{x}_0, t) - \frac{1}{c^2}\frac{\partial^2 h(\boldsymbol{x},\boldsymbol{x}_0,t)}{\partial t^2} = -\delta(\boldsymbol{x} - \boldsymbol{x}_0)\delta(t), \tag{3}$$

where δ denotes the Dirac delta function.

2.2. Boundary condition

Let us now consider a connected domain $V \subset \mathbb{R}^3$, whose boundary ∂V is a Lipschitz continuous 2D manifold (i.e. ∂V is locally the graph of a Lipschitz function). The boundary ∂V is characterized by the *specific admittance* $\widehat{\beta}(\boldsymbol{x}, k) \in \mathbb{C}$, which is an essentially bounded function of the position $\boldsymbol{x} \in \partial V$. Then Robin's boundary condition of Eq. (2) states that

$$\forall \boldsymbol{x} \in \partial V,\ \frac{\partial \varphi(\boldsymbol{x},k)}{\partial \boldsymbol{n}(\boldsymbol{x})} + 2\imath\pi k\widehat{\beta}(\boldsymbol{x},k)\varphi(\boldsymbol{x},k) = 0, \quad (4)$$

where $\frac{\partial}{\partial \boldsymbol{n}(\boldsymbol{x})}$ denotes partial differentiation in the direction of the outward normal $\boldsymbol{n}(\boldsymbol{x})$ to the boundary surface at $\boldsymbol{x}$. This boundary condition explicitly depends on k, so Eq. (2) has to be rewritten $\Delta\varphi(\boldsymbol{x},k) + 4\pi^2\kappa(k)^2\varphi(\boldsymbol{x},k) = 0$, where the wave number is now denoted $\kappa(k) \in \mathbb{C}$. In the case of *non-rigid* surfaces, which absorb a part of the energy of the incident wave, $\widehat{\beta}(\boldsymbol{x},k) \in \mathbb{C}$ and $\mathrm{Re}(\widehat{\beta}(\boldsymbol{x},k)) > 0$. Then it was proved in [8] that when the domain V is bounded, the set of eigenfunctions and generalized eigenfunctions of the complex Robin Laplacian is discrete and can be chosen to form a pseudo-orthonormal *Abel basis with brackets* of the Hilbert space $L^2(V)$, a notion that is defined in [8, Sec. III A]. However, when there is no energy absorption, $\widehat{\beta}(\boldsymbol{x},k)$ is purely imaginary, the Robin Laplacian is self-adjoint, and the set of eigenfunctions forms an orthonormal basis of $L^2(V)$. In particular, when $\widehat{\beta}(\boldsymbol{x},k) = 0$, Eq. (4) reduces to Neumann's boundary condition.

3. Fundamentals of the theory

3.1. Mathematical assumptions

The statistical wave field theory relies on three mathematical assumptions:

- Assumption 1: the source's position is a random variable uniformly distributed in V;
- Assumption 2: the frequency f (or equivalently the wave number k) is large;
- Assumption 3: the mean and pseudo-covariances of the wave field are stationary.

The first assumption turns the RIR $h(\boldsymbol{x},\boldsymbol{x}_0,t)$ introduced in Eq. (3) into a random process. The second assumption is directly related to the semiclassical approximation of quantum physics [9]. Last, the third assumption implies that the wave field statistics are independent of the receiver's position when there is no energy absorption. Under these three assumptions, the statistical wave field theory shows that the RIR $h(\boldsymbol{x},\boldsymbol{x}_0,t)$ is a centered random process. We refer the reader to [3, Sec. IV B] for more detailed explanations.

3.2. Cross-Wigner distribution

When there is energy absorption at the domain's boundary, the RIR $h(\boldsymbol{x},\boldsymbol{x}_0,t)$ defined in Sec. 2.1 is modeled as a non-stationary random process, due to the exponential damping of the eigenmodes over time. In signal processing, the standard tool for characterizing the second-order statistics of a non-stationary random process is the *Wigner distribution* [10], also known as the Wigner-Ville distribution, which describes how the power of this random process is distributed in the time-frequency plane. Let $\Gamma_h(\boldsymbol{x}_1,\boldsymbol{x}_2,\boldsymbol{x}_0,t_1,t_2) = \mathrm{cov}[h(\boldsymbol{x}_1,\boldsymbol{x}_0,t_1), h(\boldsymbol{x}_2,\boldsymbol{x}_0,t_2)]$ denote the *auto-covariance function* (ACF) of the non-stationary random process $h(\boldsymbol{x},\boldsymbol{x}_0,t)$, where $\boldsymbol{x},\boldsymbol{x}_0 \in V$ and $t \in \mathbb{R}$. Its *cross-Wigner distribution* W_h is then defined as follows: $\forall \boldsymbol{x}_1,\boldsymbol{x}_2,\boldsymbol{x}_0 \in V$, $\forall f,t \in \mathbb{R}$,

$$\begin{aligned} & W_h(\boldsymbol{x}_1,\boldsymbol{x}_2,\boldsymbol{x}_0,f,t) \\ = \ & \int_{\mathbb{R}} \Gamma_h(\boldsymbol{x}_1,\boldsymbol{x}_2,\boldsymbol{x}_0,t+\tfrac{\tau}{2},t-\tfrac{\tau}{2})\, e^{-2\imath\pi f\tau} d\tau. \end{aligned} \quad (5)$$

The cross-Wigner distribution $W_h(\boldsymbol{x}_1,\boldsymbol{x}_2,\boldsymbol{x}_0,f,t)$ in Eq. (5) can be interpreted as the covariance of the random process h between two positions $\boldsymbol{x}_1$ and $\boldsymbol{x}_2$, at fixed source position $\boldsymbol{x}_0$, frequency f and time t.

4. Isotropic wave fields

The original version of the statistical wave field theory published in [1], [5] focuses on *mixing* rooms. In these rooms, when there is no energy absorption (i.e. when $\widehat{\beta}(\boldsymbol{x},k)$ is purely imaginary), the wave field is *diffuse*, which means that its statistics are invariant over space under any translation (it is *stationary*), and any rotation (it is *isotropic*). When on the contrary there is energy absorption, then the sound power decreases exponentially over time, at a rate that is uniform in the room and depends on the frequency. The *reverberation time*, often denoted T_{60}, is then defined as the time it takes for the sound pressure level to reduce by 60 dB. An asymptotic reverberation time can also be defined in ergodic rooms that are not mixing [11].

4.1. Power distribution

4.1.1. Neumann's boundary condition

Neumann's boundary condition corresponds to the particular case of rigid surfaces ($\widehat{\beta}(\boldsymbol{x},k) = 0$). In this case, the first order asymptotic expansion of the cross-Wigner distribution $W_h(\boldsymbol{x}_1,\boldsymbol{x}_2,\boldsymbol{x}_0,f,t)$, which holds when $f \to +\infty$, was established in [1, Sec. V]:

$$W_h(\boldsymbol{x}_1,\boldsymbol{x}_2,\boldsymbol{x}_0,f,t) = W_h(f)\,\gamma(\boldsymbol{x}_1,\boldsymbol{x}_2,f), \quad (6)$$

where $W_h(f)$ is the stationary power spectral density at frequency f and at any point $\boldsymbol{x} \in V$:

$$W_h(f) = \frac{c^3\widehat{\Gamma}_B(\frac{f}{c})}{16\pi^2 f^2} = \frac{\lambda c}{4\pi}\left(1 + \frac{\lambda c S(\partial V)}{8f}\right), \quad (7)$$

and $\widehat{\Gamma}_B(k)$ is the stationary *power spectrum*:

$$\widehat{\Gamma}_B(k) = 4\pi\lambda\left(k^2 + \frac{\lambda S(\partial V)}{8}k\right). \quad (8)$$

In Eqs. (7)-(8), $\lambda = \frac{1}{|V|}$ is the inverse of the room's volume $|V|$, and $S(\partial V)$ is the area of the room's boundary surface ∂V. Eq. (7) shows that $W_h(f)$ tends to a finite value $\frac{\lambda c}{4\pi}$ when $f \to +\infty$, so we retrieve the well-known property that the RIR behaves like white noise [12]. The spectral correlation $\gamma(\boldsymbol{x}_1,\boldsymbol{x}_2,f)$ in Eq. (6) is expressed as

$$\gamma(\boldsymbol{x}_1,\boldsymbol{x}_2,f) = \mathrm{sinc}\left(\frac{2\pi f\|\boldsymbol{x}_1-\boldsymbol{x}_2\|_2}{c}\right). \quad (9)$$

We thus retrieve the usual expression of the spectral correlation in a diffuse acoustic field [13].

4.1.2. Robin's boundary condition

In the general case of Robin's boundary condition, the first order asymptotic expansion of the cross-Wigner distribution $W_h(\boldsymbol{x}_1, \boldsymbol{x}_2, \boldsymbol{x}_0, f, t)$, which holds when $f \to +\infty$, was established in [1, Sec. VI][1,2]:

$$W_h(\boldsymbol{x}_1, \boldsymbol{x}_2, \boldsymbol{x}_0, f, t) = W_h(\boldsymbol{x}_1, \boldsymbol{x}_2, \boldsymbol{x}_0, f)\, e^{-2\alpha(\frac{f}{c})t}, \tag{10}$$

where $\alpha(k) = 2\pi c\, \mathrm{Im}(\kappa(k))$ is the spectral attenuation, and $\kappa(k)$ is the complex wave numbers distortion:

$$\begin{aligned}\kappa(k) = \quad & k + \tfrac{\imath\lambda}{8\pi} \int_{\boldsymbol{s}\in\partial V} \Bigg(\ln\left(\tfrac{1+\widehat{\beta}(\boldsymbol{s},k)}{1-\widehat{\beta}(\boldsymbol{s},k)}\right) \\ & -\widehat{\beta}(\boldsymbol{s},k)^2 \ln\left(\tfrac{\widehat{\beta}(\boldsymbol{s},k)+1}{\widehat{\beta}(\boldsymbol{s},k)-1}\right) + 2\widehat{\beta}(\boldsymbol{s},k)\Bigg) dS(\boldsymbol{s}),\end{aligned} \tag{11}$$

where dS denotes the surface measure. We note that $W_h(\boldsymbol{x}_1, \boldsymbol{x}_2, \boldsymbol{x}_0, f, t)$ in Eq. (10) has the same factorized form as the Polack time-frequency distribution [14] (which was originally known only for $\boldsymbol{x}_1 = \boldsymbol{x}_2$).

In Eq. (10), when the variations of the power distribution over space are negligible (i.e., when $\mathrm{Re}(\widehat{\beta}(\boldsymbol{x}, k))$ is small), $W_h(\boldsymbol{x}_1, \boldsymbol{x}_2, \boldsymbol{x}_0, f)$ can be written as

$$W_h(\boldsymbol{x}_1, \boldsymbol{x}_2, \boldsymbol{x}_0, f) = W_h(f)\, \gamma(\boldsymbol{x}_1, \boldsymbol{x}_2, f), \tag{12}$$

where $W_h(f)$ is the stationary power distribution:

$$W_h(f) = \frac{c^3 \widehat{\Gamma}_\kappa(\frac{f}{c})}{4\left(4\pi^2 f^2 + \alpha(\frac{f}{c})^2\right)}, \tag{13}$$

which generalizes Eq. (7), $\gamma(\boldsymbol{x}_1, \boldsymbol{x}_2, f)$ is the spectral correlation defined in Eq. (9), and $\widehat{\Gamma}_\kappa(k) = \frac{\widehat{\Gamma}_B((\mathrm{Re}\kappa)^{-1}(k))}{(\mathrm{Re}\kappa)'((\mathrm{Re}\kappa)^{-1}(k))}$ is the distorted power spectrum that generalizes Eq. (8).

4.2. Reverberation time

Equation (11) yields the expression of the reverberation time in ergodic rooms, which holds for all values of the specific admittance, and which can be written in exactly the same form as Eyring's formula [15]:

$$T_{60}(f) = \frac{3\ln(10)}{\alpha(\frac{f}{c})} = \frac{24\ln(10)}{c} \frac{|V|}{-\int_{\boldsymbol{s}\in\partial V} \ln(1-a(\boldsymbol{s},f))dS(\boldsymbol{s})}, \tag{14}$$

where $a(\boldsymbol{s}, f)$ denotes the absorption coefficient averaged over all angles of incidence:

$$a(\boldsymbol{s}, f) = 1 - \exp\left(\frac{\int_{u=0}^{1} \ln\left(1-a(\boldsymbol{s},\frac{f}{c},u)\right) u\, du}{\int_{u=0}^{1} u\, du}\right), \tag{15}$$

and $a(\boldsymbol{s}, k, u)$ is the absorption for an incident plane wave of frequency ck and angle θ, such that $u = \cos(\theta)$:

$$a(\boldsymbol{s}, k, u) = 1 - \left|\frac{u-\widehat{\beta}(\boldsymbol{s},k)}{u+\widehat{\beta}(\boldsymbol{s},k)}\right|^2. \tag{16}$$

In [5], we remarked that at high frequency, the reverberation time in Eq. (14) is lower bounded, independently of the specific admittance, by a constant that depends on the room geometry only through its volume and the area of its boundary surface[3,4]:

$$T_{60}(f) \geq \frac{24\ln(10)}{4.7987} \frac{|V|}{c\, S(\partial V)} \approx \frac{11.5160\, |V|}{c\, S(\partial V)}. \tag{17}$$

4.3. Experimental verification

In [6], the formula of the reverberation time in Eq. (14) was compared to various model predictions. For a simulated shoebox room, a good agreement has been found between the modal model [17], diffusion-equation model [18], and Eq. (14), both as a function of frequency and as a function of complex-valued impedance, even though this room is not ergodic. For a simulated ergodic reverberation chamber, good agreement has also been found between the Helmholtz model [19], diffusion-equation model [18], and Eq. (14). The convergence of the solutions with increasing frequency and impedance confirms that Eq. (14) effectively predicts the reverberation time in an ergodic room, based on the room's volume, surface area, and surface impedance. Additionally, the statistical wave field theory has been used to estimate the impedance of surfaces in both a real shoebox-shaped room and a real reverberation chamber [6].

4.4. Curvature term

In [5], the closed-form expression of the reverberation time in Eq. (14) was refined by taking the curvature of the boundary surface into account, resulting in a new term in the denominator, which decreases as $\frac{c}{f}$:

$$T_{60}(f) = \frac{24\ln(10)}{c} \times \frac{|V|}{\mathrm{Re}\left(\epsilon_1(\frac{f}{c})\right) + \frac{c}{f}\left(\mathrm{Im}\left(\epsilon_2(\frac{f}{c}) - \frac{\lambda\epsilon_1(\frac{f}{c})^2}{16\pi}\right) - \frac{\lambda S(\partial V)}{8}\mathrm{Re}\left(\epsilon_1(\frac{f}{c})\right)\right)} \tag{18}$$

where functions $\epsilon_1(.)$ and $\epsilon_2(.)$ are defined as

[1] The equations in Secs. 4.1.2, 4.2, 5.3.2 and 5.4 are simplified expressions that hold provided that $\lim_{k\to+\infty} d\widehat{\beta}(\boldsymbol{s}, k)/dk = 0$. When this condition is not satisfied, the theory leads to implicit equations that need to be solved numerically.

[2] Actually, the expression of the Wigner distribution provided in [1, Sec. VI] was that of the time derivative of the RIR, $q = \frac{\partial h}{\partial t}$. In Sec. 4.1.2, we provide the Wigner distribution of the RIR h.

[3] At first sight, this remark may seem surprising, because Eyring's formula is known to allow the reverberation time to be zero when the average absorption coefficient is 1 on a portion of the boundary of positive measure [15]. This apparent contradiction is resolved by noting that the expression of the absorption coefficient in Eq. (15) is averaged over all possible directions of incidence; however, the angle-dependent absorption coefficient in Eq. (16) can only reach the maximal value of 1 at a single angle of incidence. Therefore the average absorption coefficient is upper bounded by a value that is strictly lower than 1, everywhere on the boundary ∂V.

[4] The lower bound in Eq. (17) was established by assuming that the room has *locally reacting* boundary surfaces, which means that $\widehat{\beta}$ depends only on the position $\boldsymbol{s} \in \partial V$ and on the wave number k, but not on the angle of sound incidence. Consequently, this inequality might be violated in the case non-locally reacting room surfaces. In practice, surfaces with local reaction are rather the exception than the rule [16, Chap. 2].

$$\epsilon_1(k) = 2\int_{s\in\partial V}\Big(\ln\Big(\frac{1+\widehat{\beta}(\boldsymbol{s},k)}{1-\widehat{\beta}(\boldsymbol{s},k)}\Big)+2\widehat{\beta}(\boldsymbol{s},k) -\widehat{\beta}(\boldsymbol{s},k)^2\ln\Big(\frac{\widehat{\beta}(\boldsymbol{s},k)+1}{\widehat{\beta}(\boldsymbol{s},k)-1}\Big)\Big)dS(\boldsymbol{s}), \quad (19)$$

$$\epsilon_2(k) = \int_{s\in\partial V}\frac{1}{2\pi\widehat{\beta}(\boldsymbol{s},k)}\Big(\ln\Big(\frac{1+\widehat{\beta}(\boldsymbol{s},k)}{1-\widehat{\beta}(\boldsymbol{s},k)}\Big)-2\widehat{\beta}(\boldsymbol{s},k) +\widehat{\beta}(\boldsymbol{s},k)^2\ln\Big(\frac{\widehat{\beta}(\boldsymbol{s},k)+1}{\widehat{\beta}(\boldsymbol{s},k)-1}\Big)\Big)\Big(\frac{1}{R_1(\boldsymbol{s})}+\frac{1}{R_2(\boldsymbol{s})}\Big)dS(\boldsymbol{s}). \quad (20)$$

Indeed, the term $\epsilon_2(.)$ defined in Eq. (20) explicitly depends on the two *main curvature radii* $R_1(\boldsymbol{s})$ and $R_2(\boldsymbol{s})$ at any point $\boldsymbol{s}$ of the boundary surface ∂V [20]. When $f \to +\infty$, the term that is proportional to $\frac{c}{f}$ in the denominator of Eq. (18) can be neglected; then this equation reduces to Eq. (14). We thus conclude that the accuracy of Eq. (18) is improved at lower frequencies compared to Eq. (14).

5. Anisotropic wave fields

In [3], we defined the general classes of *semi-ergodic* and *semi-mixing* rooms, which generalize the ergodic and mixing rooms addressed in Sec. 4. In particular, the class of semi-ergodic rooms includes all ergodic rooms and all (possibly non-convex) polyhedra. We showed that, when there is no energy absorption, the wave field in semi-mixing rooms is approximately stationary, but it is generally not isotropic. Then in [4], we showed that when on the contrary there is energy absorption, the wave field is characterized by a *directional reverberation time* that is independent of the receiver's position, but depends on its orientation.

5.1. Special polyhedra

In [2], we introduced a simple geometric approach to the statistical wave field theory dedicated to a few polyhedra including the rectangular cuboid, whose statistical properties are related to mathematical crystallography. These *special polyhedra* are not ergodic, but rather *integrable*, which means that the Helmholtz equation can be solved in closed-form subject to various boundary conditions (Dirichlet, Neumann, and even Robin in certain cases). Moreover, all the eigenfunctions are trigonometric polynomials. Based on these closed-form solutions, deriving the equations of the theory proved to be much easier than in the ergodic case. In addition, the high frequency approximation was not even required: the theory predictions hold right from the zero frequency.

5.2. Directional measure

The wave field in any semi-ergodic room is characterized by a *directional measure* $\sigma(.|\boldsymbol{v})$ defined on the set $\mathcal{S}(0,1)$ of all unitary vectors, which can be interpreted as the probability distribution of the directions taken over time by almost every ray trajectory in the corresponding classical billiard, where $\boldsymbol{v} \in \mathcal{S}(0,1)$ denotes the initial direction of the ray at $t = 0$. The example of the rectangular billiard, where almost every ray trajectory takes only four different directions, is illustrated in Fig. 1. In the same way, in all special polyhedra, the support of σ is discrete and includes $\boldsymbol{v}$. In ergodic rooms, on the contrary, the measure σ is uniform on $\mathcal{S}(0,1)$, for almost all $\boldsymbol{v} \in \mathcal{S}(0,1)$.

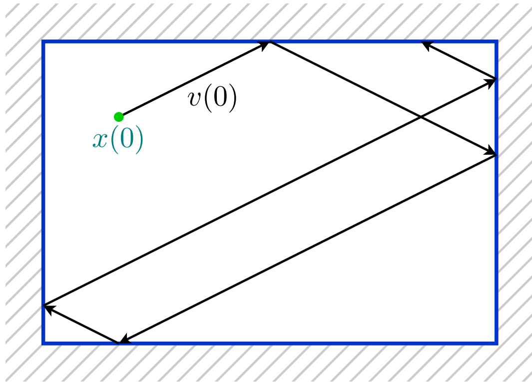

Figure 1: Example of ray trajectory in the rectangular billiard (from [3]). The discrete directional measure σ assigns the same weight to the four directions taken by the ray trajectory, including $\boldsymbol{v}(0)$. The trajectory is interrupted after six reflections to avoid overloading the figure, but after that it will explore space uniformly over time.

In the general case of semi-ergodic billiards, the directional measure σ was characterized as follows in [3, Sec. III]. For all $l \in \mathbb{N}$, let $\boldsymbol{Y}_l$ denote the $(2l+1)$-dimensional column vector of coefficients $Y_{l,m}$, where $\forall m \in \{-l,\dots,l\}$, $Y_{l,m}$ denotes the real spherical harmonic of degree l and order m [21]. Then $\forall l \in \mathbb{N}$, let $\boldsymbol{A}_l$ be the $(2l+1)\times(2l+1)$ real symmetric positive semidefinite matrix

$$\boldsymbol{A}_l = \lambda\int_{\partial V}\Big(\boldsymbol{I} - \Big(\int_{\boldsymbol{u}\in\mathcal{S}(0,1)}\boldsymbol{Y}_l(\boldsymbol{u})\times \boldsymbol{Y}_l\left(\boldsymbol{u}-2(\boldsymbol{n}(\boldsymbol{s})^\top\boldsymbol{u})\boldsymbol{n}(\boldsymbol{s})\right)^\top dS(\boldsymbol{u})\Big)\Big)dS(\boldsymbol{s}), \quad (21)$$

where $\boldsymbol{I}$ is the identity matrix. Then $\forall \boldsymbol{v} \in \mathcal{S}(0,1)$, the directional measure $\sigma(S|\boldsymbol{v})$ of any measurable subset S of the unit sphere $\mathcal{S}(0,1)$ is expressed as

$$\sigma(S|\boldsymbol{v}) = \lim_{L\to+\infty}\int_{\boldsymbol{u}\in S}\sigma_L(\boldsymbol{u},\boldsymbol{v})dS(\boldsymbol{u}), \quad (22)$$

where $\forall L \in \mathbb{N}$,

$$\sigma_L(\boldsymbol{u},\boldsymbol{v}) = \sum_{l=0}^{L}\boldsymbol{Y}_l(\boldsymbol{v})^\top \mathrm{Proj}_{\mathrm{Ker}(\boldsymbol{A}_l)}\boldsymbol{Y}_l(\boldsymbol{u}), \quad (23)$$

and $\mathrm{Proj}_{\mathrm{Ker}(\boldsymbol{A}_l)}$ denotes the orthogonal projection matrix onto the kernel of matrix $\boldsymbol{A}_l$ defined in Eq. (21). Since the series expansion over spherical harmonics in Eq. (23) is truncated to degree L, $\boldsymbol{u} \mapsto \sigma_L(\boldsymbol{u},\boldsymbol{v})$ can be interpreted as a smooth density function over $\mathcal{S}(0,1)$, which can be equivalently obtained by smoothing the (possibly discrete) directional measure σ in Eq. (22), over the set of unit direction vectors $\boldsymbol{u} \in \mathcal{S}(0,1)$.

5.3. Power distribution

5.3.1. Neumann's boundary condition

In the case of Neumann's boundary condition, the first order asymptotic expansion of the cross-Wigner distribution $W_h(\boldsymbol{x}_1, \boldsymbol{x}_2, \boldsymbol{x}_0, f, t)$, which holds when $f \to +\infty$, was established in [3, Sec. V]:

$$\begin{aligned} & W_h(\boldsymbol{x}_1, \boldsymbol{x}_2, \boldsymbol{x}_0, f, t) \\ = \; & \tfrac{c^3}{16\pi^2 f^2} \int_{\boldsymbol{k} \in \mathcal{S}(0, \frac{f}{c})} \cos(2\pi \boldsymbol{k}^\top (\boldsymbol{x}_1 - \boldsymbol{x}_2)) \widehat{\Gamma}_L(\boldsymbol{k}) dS(\boldsymbol{k}), \end{aligned} \tag{24}$$

where $\boldsymbol{k}$ denotes the wave vector, $\mathcal{S}(0, k)$ is the sphere centered at the origin and of radius $k = \|\boldsymbol{k}\|_2$, and $\widehat{\Gamma}_L(\boldsymbol{k})$ is the stationary power spectrum:

$$\begin{aligned} \widehat{\Gamma}_L(\boldsymbol{k}) = \; & \lambda \Big(1 + \tfrac{\lambda}{4} \int_{\boldsymbol{s} \in \partial V} \Big(\int_{\boldsymbol{u} \in \mathcal{S}(0,1)} \\ & \delta \left(\boldsymbol{u}^\top \boldsymbol{k} \right) \, \sigma_L(\boldsymbol{u}, \boldsymbol{n}(\boldsymbol{s})) \, dS(\boldsymbol{u}) \Big) dS(\boldsymbol{s}) \Big). \end{aligned} \tag{25}$$

When $\boldsymbol{x}_1 = \boldsymbol{x}_2 = \boldsymbol{x}$, we retrieve the same expression of the stationary power distribution $W_h(\boldsymbol{x}, \boldsymbol{x}, \boldsymbol{x}_0, f, t)$ as in isotropic wave fields: $W_h(\boldsymbol{x}, \boldsymbol{x}, \boldsymbol{x}_0, f, t) = W_h(f)$, where $W_h(f)$ was defined in Eq. (7). However, Eq. (24) is different from Eq. (6), which shows that the spectral correlation in anisotropic wave fields is generally different from Eq. (9) that holds in the diffuse case.

5.3.2. Robin's boundary condition

In the general case of Robin's boundary condition, when the variations of the power distribution over space are negligible (i.e., when $\mathrm{Re}(\widehat{\beta}(\boldsymbol{x}, k))$ is small), then the first order asymptotic expansion of the cross-Wigner distribution $W_h(\boldsymbol{x}_1, \boldsymbol{x}_2, \boldsymbol{x}_0, f, t)$, which holds when $f \to +\infty$, was established in [4, Sec. VI]:

$$\begin{aligned} W_h(\boldsymbol{x}_1, \boldsymbol{x}_2, \boldsymbol{x}_0, f, t) = \; & \tfrac{c^3}{4} \int_{\boldsymbol{k} \in \mathcal{S}(0, \frac{f}{c})} e^{2\imath\pi \boldsymbol{k}^\top (\boldsymbol{x}_1 - \boldsymbol{x}_2)} \\ & \tfrac{e^{-2\alpha_L(\boldsymbol{k}) t}}{4\pi^2 f^2 + \alpha_L(\boldsymbol{k})^2} \, \widehat{\Gamma}_{\boldsymbol{\kappa}_L}(\boldsymbol{k}) \, dS(\boldsymbol{k}), \end{aligned} \tag{26}$$

where $\alpha_L(\boldsymbol{k}) = 2\pi c \, \mathrm{Im}(\kappa_L(\boldsymbol{k}))$ is the spectral attenuation, $\kappa_L(\boldsymbol{k}) = \frac{\boldsymbol{k}^\top \boldsymbol{\kappa}_L(\boldsymbol{k})}{\|\boldsymbol{k}\|_2}$ is the wave numbers distortion, and $\boldsymbol{\kappa}_L(\boldsymbol{k})$ is the complex wave vectors distortion:

$$\begin{aligned} & \boldsymbol{\kappa}_L(\boldsymbol{k}) = \boldsymbol{k} + \imath \tfrac{\lambda}{4\pi} \int_{\boldsymbol{s} \in \partial V} \int_{\boldsymbol{u} \in \mathcal{S}(0,1)} \\ & \boldsymbol{u} \ln \left(\tfrac{\boldsymbol{u}^\top \boldsymbol{k} + \|\boldsymbol{k}\|_2 \widehat{\beta}(\boldsymbol{s}, \|\boldsymbol{k}\|_2)}{\boldsymbol{u}^\top \boldsymbol{k} - \|\boldsymbol{k}\|_2 \widehat{\beta}(\boldsymbol{s}, \|\boldsymbol{k}\|_2)} \right) \sigma_L(\boldsymbol{u}, \boldsymbol{n}(\boldsymbol{s})) \, dS(\boldsymbol{u}) dS(\boldsymbol{s}), \end{aligned} \tag{27}$$

where σ_L was expressed in Eq. (23). In Eq. (26), $\widehat{\Gamma}_{\boldsymbol{\kappa}_L}(\boldsymbol{k}) = \frac{\widehat{\Gamma}_L\left((\mathrm{Re}\, \boldsymbol{\kappa}_L)^{-1}(\boldsymbol{k})\right)}{\left|\det\left(\mathrm{Jac}_{\mathrm{Re}\, \boldsymbol{\kappa}_L}\left((\mathrm{Re}\, \boldsymbol{\kappa}_L)^{-1}(\boldsymbol{k})\right)\right)\right|}$ generalizes Eq. (25). Finally, when $\boldsymbol{x}_1 = \boldsymbol{x}_2 = \boldsymbol{x}$, Eq. (26) yields the power distribution over space, frequency and time:

$$\begin{aligned} & W_h(\boldsymbol{x}, \boldsymbol{x}, \boldsymbol{x}_0, f, t) \\ = \; & \tfrac{c^3}{4} \int_{\boldsymbol{k} \in \mathcal{S}(0, \frac{f}{c})} \tfrac{e^{-2\alpha_L(\boldsymbol{k}) t}}{4\pi^2 f^2 + \alpha_L(\boldsymbol{k})^2} \, \widehat{\Gamma}_{\boldsymbol{\kappa}_L}(\boldsymbol{k}) \, dS(\boldsymbol{k}). \end{aligned} \tag{28}$$

In the case of mixing rooms, we showed in Sec. 4.1.2 that the cross-Wigner distribution $W_h(\boldsymbol{x}_1, \boldsymbol{x}_2, \boldsymbol{x}_0, f, t)$ was factorizable as the product of a function of space and a function of time at fixed frequency f, as in Polack's formula [14]. So, the power distribution at any frequency f decreases exponentially over time. However, in the anisotropic case, $W_h(\boldsymbol{x}_1, \boldsymbol{x}_2, \boldsymbol{x}_0, f, t)$ in Eq. (26) is a linear combination of infinitely many decreasing exponentials. We thus retrieve a well-known fact in room acoustics: the time decay in non-ergodic rooms is not exponential [16].

5.4. Reverberation time

Equation (27) permits us to establish a novel result: the closed-form expression of the directional reverberation time in semi-ergodic rooms, which holds for all values of the specific admittance:

$$\begin{aligned} & T_{60}(\boldsymbol{k}) = \tfrac{3 \ln(10)}{\alpha_L(\boldsymbol{k})} = \tfrac{24 \ln(10)}{c} \times \\ & \frac{|V|}{\left(\begin{array}{c} -2 \int_{\boldsymbol{s} \in \partial V} \int_{\boldsymbol{u} \in \mathcal{S}(0,1)} \ln\left(1 - a\left(\boldsymbol{s}, \|\boldsymbol{k}\|_2, \frac{|\boldsymbol{u}^\top \boldsymbol{k}|}{\|\boldsymbol{k}\|_2}\right)\right) \\ \times \frac{|\boldsymbol{u}^\top \boldsymbol{k}|}{\|\boldsymbol{k}\|_2} \sigma_L(\boldsymbol{u}, \boldsymbol{n}(\boldsymbol{s})) dS(\boldsymbol{u}) dS(\boldsymbol{s}) \end{array} \right)} \end{aligned} \tag{29}$$

where $a(\boldsymbol{s}, k, u)$ and $\sigma_L(\boldsymbol{u}, \boldsymbol{v})$ were expressed in Eqs. (16) and (23). Physically, Eq. (29) can be interpreted as follows: for a plane wave of wave vector $\boldsymbol{k}$ and for any point $\boldsymbol{s} \in \partial V$ on the boundary surface,

- the outward normal $\boldsymbol{n}(\boldsymbol{s})$ of the boundary surface at $\boldsymbol{s}$ is seen, through the successive reflections of the plane wave over the boundary surface, as a random vector $\boldsymbol{u} \in \mathcal{S}(0,1)$, of probability density function $\sigma_L(\boldsymbol{u}, \boldsymbol{n}(\boldsymbol{s}))$ over $\mathcal{S}(0,1)$;
- the angle of incidence θ of the plane wave on the boundary surface at $\boldsymbol{s}$ is such that $\cos(\theta) = \frac{\boldsymbol{u}^\top \boldsymbol{k}}{\|\boldsymbol{k}\|_2}$;
- $|\cos(\theta)| dS(\boldsymbol{s})$ is the apparent area of the surface element $dS(\boldsymbol{s})$ for the plane wave;
- $a(\boldsymbol{s}, \|\boldsymbol{k}\|_2, |\cos(\theta)|) \in [0,1]$ is the absorption coefficient of the boundary surface at point $\boldsymbol{s}$, frequency $f = c\|\boldsymbol{k}\|_2$, and angle θ.

Note that Eq. (29) can be rewritten in the same form as Eyring's formula [15] as expressed in Eq. (14), except that $T_{60}(\boldsymbol{k})$ depends not only on the norm of wave vector $\boldsymbol{k}$, but also on its direction:

$$T_{60}(\boldsymbol{k}) = \tfrac{24 \ln(10)}{c} \frac{|V|}{- \int_{\boldsymbol{s} \in \partial V} \ln(1 - a(\boldsymbol{s}, \boldsymbol{k})) dS(\boldsymbol{s})}, \tag{30}$$

with the average directional absorption coefficient

$$\begin{aligned} & a(\boldsymbol{s}, \boldsymbol{k}) = 1 - \\ & e^{2 \int_{\boldsymbol{u} \in \mathcal{S}(0,1)} \ln\left(1 - a\left(\boldsymbol{s}, \|\boldsymbol{k}\|_2, \frac{|\boldsymbol{u}^\top \boldsymbol{k}|}{\|\boldsymbol{k}\|_2}\right)\right) \frac{|\boldsymbol{u}^\top \boldsymbol{k}|}{\|\boldsymbol{k}\|_2} \sigma_L(\boldsymbol{u}, \boldsymbol{n}(\boldsymbol{s})) \, dS(\boldsymbol{u})}, \end{aligned} \tag{31}$$

which involves a geometric mean over all angles of incidence. In the isotropic case, $\sigma_L(\boldsymbol{u}, \boldsymbol{v}) = \frac{1}{4\pi}$, then $T_{60}(\boldsymbol{k})$ and $a(\boldsymbol{s}, \boldsymbol{k})$ depend only on $k = \|\boldsymbol{k}\|_2$, and Eqs. (30) and (31) reduce exactly to Eqs. (14) and (15), respectively. Conversely, in the particular case of the rectangular cuboid, Eq. (29) reduces to Eq. (34) in [22] when $L \to +\infty$. In addition, in the general anisotropic case, when the average directional absorption coefficient $a(\boldsymbol{s}, \boldsymbol{k})$ is small, Eqs. (30) and (31) yield

$$T_{60}(\boldsymbol{k}) = \tfrac{24 \ln(10)}{c} \frac{|V|}{\int_{\boldsymbol{s} \in \partial V} a(\boldsymbol{s}, \boldsymbol{k}) dS(\boldsymbol{s})} \tag{32}$$

$$a(\boldsymbol{s},\boldsymbol{k}) = \begin{array}{l} 2\int_{\boldsymbol{u}\in\mathcal{S}(0,1)} a\left(\boldsymbol{s},\|\boldsymbol{k}\|_2,\frac{|\boldsymbol{u}^\top\boldsymbol{k}|}{\|\boldsymbol{k}\|_2}\right) \\ \times\frac{|\boldsymbol{u}^\top\boldsymbol{k}|}{\|\boldsymbol{k}\|_2}\sigma_L(\boldsymbol{u},\boldsymbol{n}(\boldsymbol{s}))\,dS(\boldsymbol{u}),\end{array} \quad (33)$$

which now involves an arithmetic mean over all angles of incidence. Then, again in the particular isotropic case, $T_{60}(\boldsymbol{k})$ and $a(\boldsymbol{s},\boldsymbol{k})$ depend only on $k = \|\boldsymbol{k}\|_2$, and Eq. (32) reduces exactly to Sabine's formula [1, Eq. (40)]. Moreover, Eq. (33) can be rewritten in the form $a(\boldsymbol{s},k) = \int_{\theta=0}^{\frac{\pi}{2}} a(\boldsymbol{s},k,\cos(\theta))\sin(2\theta)\,d\theta$, which is exactly the *Paris* formula of the average absorption coefficient for a random, uniformly and isotropically distributed sound incidence, as expressed in [16, p. 55] and [7, p. 580]. We can thus conclude that Eq. (31) is both more accurate and more general than the Paris formula, because it also holds at higher absorption and in anisotropic wave fields.

6. Conclusion

In summary, the statistical wave field theory brings various contributions to the field of room acoustics:

- it provides a *unified framework* that encompasses the previously known statistical properties of late reverberation in mixing rooms (Sec. 4);
- it provides a *global description* of the wave field, through the closed-form expression of its power distribution and correlations over time, frequency and space (Secs. 4.1 and 5.3);
- it is applicable to a *large class of room shapes* that generate anisotropic wave fields (Sec. 5);
- it is *more accurate* than the existing approaches thanks to the semiclassical approximation of quantum physics (Sec. 3.1), which e.g. accounts for the curvature of the boundary (Sec. 4.4);
- finally, in addition to the results presented in this paper, it reveals the existence of *black holes*, which behave like those of general relativity: a part of the sound energy may be trapped in the vicinity of the domain's boundary [4, Sec. VI C].

Moreover, the predicted reverberation time in ergodic rooms has been *verified by experiment* (Sec. 4.3). We believe that this theory may find many applications in room acoustics, including artificial reverberation and impedance measurement of materials in a room.

References

[1] R. Badeau, "Statistical wave field theory," *J. Acoust. Soc. Am.*, vol. 156, no. 1, pp. 573–599, Jul. 2024.

[2] R. Badeau, "Statistical wave field theory: Special polyhedra," *J. Acoust. Soc. Am.*, vol. 157, no. 3, pp. 2263–2278, Mar. 2025.

[3] R. Badeau, "Statistical wave field theory: Anisotropic wave fields under Neumann's boundary condition," *J. Acoust. Soc. Am.*, vol. 159, no. 3, pp. 2265–2280, Mar. 2026.

[4] R. Badeau, "Statistical wave field theory: Anisotropic wave fields under Robin's boundary condition," *J. Acoust. Soc. Am.*, vol. 159, no. 6, pp. 5359–5377, Jun. 2026.

[5] R. Badeau, "Statistical wave field theory: Curvature term," *J. Acoust. Soc. Am.*, vol. 157, no. 3, pp. 1650–1664, Mar. 2025.

[6] A. G. Prinn and R. Badeau, "Verification of reverberation time predictions derived from the statistical wave field theory," *Applied Acoustics*, vol. 250, p. 111 337, Jun. 2026.

[7] P. M. Morse and K. U. Ingard, *Theoretical acoustics*. New York, NY, USA: McGraw-Hill, 1968.

[8] R. Badeau, "On the spectral decomposition of the complex Robin Laplacian," *J. Acoust. Soc. Am.*, vol. 158, no. 1, pp. 838–848, Jul. 2025.

[9] M. Sieber, H. Primack, U. Smilansky, I. Ussishkin, and H. Schanz, "Semiclassical quantization of billiards with mixed boundary conditions," *Journal of Physics A: Mathematical and General*, vol. 28, no. 17, pp. 5041–5078, 1995.

[10] L. Cohen, "Time-frequency distributions-a review," *Proc. IEEE*, vol. 77, no. 7, pp. 941–981, Jul. 1989.

[11] J.-D. Polack, "Modifying chambers to play billiards: The foundations of reverberation theory," *Acta Acustica united with Acustica*, vol. 76, no. 6, 256–272(17), Jul. 1992.

[12] J. A. Moorer, "About this reverberation business," *Comp. Music Journal*, vol. 3, no. 2, pp. 13–28, 1979.

[13] R. Cook, R. Waterhouse, R. Berendt, S. Edelman, and M. Thompson, "Measurement of correlation coefficients in reverberant sound fields," *The Journal of the Acoustical Society of America*, vol. 27, no. 6, pp. 1072–1077, 1955.

[14] J.-D. Polack, "La transmission de l'énergie sonore dans les salles (*The transmission of sound energy in rooms*)," Ph.D. dissertation, Université du Maine, Le Mans, France, 1988.

[15] C. F. Eyring, "Reverberation time in "dead" rooms," *The Journal of the Acoustical Society of America*, vol. 1, no. 2A, pp. 217–241, 1930.

[16] H. Kuttruff, *Room Acoustics, Fifth Edition*. Boca Raton, FL, USA: CRC Press, 2014, pp. 1–374.

[17] P. M. Morse and R. H. Bolt, "Sound waves in rooms," *Rev. Mod. Phys.*, vol. 16, pp. 69–150, 2 Apr. 1944.

[18] A. G. Prinn and E. A. P. Habets, "Diffusion equation-based estimation of spatially non-uniform surface absorption coefficients," in *Forum Acusticum*, Malaga, Spain, Jun. 2025.

[19] A. G. Prinn, "A review of finite element methods for room acoustics," *Acoustics*, vol. 5, no. 2, pp. 367–395, 2023.

[20] S. Kobayashi and K. Nomizu, *Foundations of Differential Geometry, Volume 2*. Hoboken, NJ: Wiley-Interscience, Feb. 1996.

[21] R. Courant and D. Hilbert, "Special functions defined by eigenvalue problems," in *Methods of Mathematical Physics*, John Wiley & Sons, Ltd, 1989, ch. 7, pp. 466–549.

[22] S. Bilbao and B. Alary, "Directional reverberation time and the image source method for rectangular parallelepipedal rooms," *J. Acoust. Soc. Am.*, vol. 155, no. 2, pp. 1343–1352, Feb. 2024.